12 Beck L, D'Amore P. Vascular development: Cellular and molecular regulation. *FASEB J* 1997; **11**: 365–73.
13 Seghezzi G, Patel S, Ren C *et al.* Fibroblast growth factor-2 (FGF-2) induces vascular endothelial growth factor (VEGF) expression in the endothelial cells of forming capillaries: An autocrine mechanism contributing to angiogenesis. *J Cell Biol* 1998; **141**: 1659–73.
14 Rusnati M, Tanghetti E, Urbinati C *et al.* Interaction of fibroblast growth factor-2 (FGF-2) with free gangliosides: Biochemical characterization and biological consequences in endothelial cell cultures. *Mol Biol Cell* 1999; **10**: 313–27.
15 Ahmed NU, Ueda M, Ito A, Ohashi A, Funasaka Y, Ichihashi M. Expression of fibroblast growth factor receptors in naevus-cell naevus and malignant melanoma. *Melanoma Res* 1997; **7**: 299–305.
16 Kato J, Wanebo H, Calabresi P, Clark JW. Basic fibroblast growth factor production and growth factor receptors as potential targets for melanoma therapy. *Melanoma Res* 1992; **2**: 13–23.
17 Lappi DA, Maher PA, Martineau D, Baird A. The basic fibroblast growth factor–saporin mitotoxin acts through the basic fibroblast growth factor receptor. *J Cell Physiol* 1991; **147**: 17–26.
18 Lappi DA, Ying W, Barthelemy I *et al.* Expression and activities of a recombinant basic fibroblast growth factor–saporin fusion protein. *J Biol Chem* 1994; **269**: 12552–8.
19 Beitz JG, Davol P, Clark JW *et al.* Antitumor activity of basic fibroblast growth factor–saporin mitotoxin *in vitro* and *in vivo*. *Cancer Res* 1992; **52**: 227–30.
20 Rybak SM, Saxena SK, Ackerman EJ, Youle RJ. Cytotoxic potential of ribonuclease and ribonuclease hybrid proteins. *J Biol Chem* 1991; **266**: 21202–7.
21 Jinno H, Ueda M, Ozawa S *et al.* Epidermal growth factor receptor-dependent cytotoxicity for human squamous carcinoma cell lines of a conjugate composed of human EGF and RNase1. *Life Sci* 1996; **58**: 1901–8.
22 Psarras K, Ueda M, Yamamura T *et al.* Human pancreatic RNase1–human epidermal growth factor fusion: an entirely human 'immunotoxin analog' with cytotoxic properties against squamous cell carcinomas. *Protein Eng* 1998; **11**: 1285–92.
23 Beintema JJ. Introduction: the ribonuclease A superfamily. *Cell Mol Life Sci* 1998; **54**: 763–5.
24 Rybak SM, Pearson JW, Fogler WE *et al.* Enhancement of vincristine cytotoxicity in drug-resistant cells by simultaneous treatment with onconase, an antitumor ribonuclease. *J Natl Cancer Inst* 1996; **88**: 747–53.
25 Jinno H, Ueda M, Ozawa S *et al.* Epidermal growth factor receptor-dependent cytotoxic effect by an EGF-ribonuclease conjugate on human cancer cell lines – a trial for less immunogenic chimeric toxin. *Cancer Chemother Pharmacol* 1996; **38**: 303–8.
26 Futami J, Seno M, Kosaka M, Tada H, Seno S, Yamada H. Recombinant human pancreatic ribonuclease produced in *E. coli*: importance of the amino-terminal sequence. *Biochem Biophys Res Commun* 1995; **216**: 406–13.
27 Futami J, Tada H, Seno M, Ishikami S, Yamada H. Stabilization of human RNase1 by introduction of a disulfide bond between residues 4 and 118. *J Biochem* 2000; **128**: 245–50.
28 Kobe B, Deisenhofer J. Mechanism of ribonuclease inhibition by ribonuclease inhibitor protein based on the crystal structure of its complex with ribonuclease A. *J Mol Biol* 1996; **264**: 1028–43.
29 Futami J, Seno M, Ueda M, Tada H, Yamada H. Inhibition of cell growth by a fused protein of human ribonuclease 1 and human basic fibroblast growth factor. *Protein Eng* 1999; **12**: 1013–19.
30 Hoshimoto S, Ueda M, Jinno H, Kitajima M, Futami J, Seno M. Mechanisms of growth inhibitory effect of RNase–EGF fused proteins against EGFR-overexpressing cells. *Anticancer Res* 2006; **26**: 857–64.
31 Tada H, Onizuka M, Muraki K *et al.* Insertional-fusion of basic fibroblast growth factor endowed ribonuclease 1 with enhanced cytotoxicity by steric blockade of inhibitor interaction. *FEBS Lett* 2004; **568**: 39–43.
32 Blanckaert VD, Schelling ME, Elstad CA, Meadows GG. Differential growth factor production, secretion, and response by high and low metastatic variants of B16BL6 melanoma. *Cancer Res* 1993; **53**: 4075–81.
33 Hayashida T, Ueda M, Aiura K *et al.* Anti-angiogenic effect of an insertional fusion protein of human basic fibroblast growth factor and ribonuclease-1. *Protein Eng Des Sel* 2005; **18**: 321–7.
34 Futami J, Tsushima Y, Tada H, Seno M, Yamada H. Convenient and efficient *in vitro* folding of disulfide-containing globular protein from crude bacterial inclusion bodies. *J Biochem* 2000; **127**: 435–41.
35 Gill SC, von Hippel PH. Calculation of protein extinction coefficients from amino acid sequence data. *Anal Biochem* 1989; **182**: 319–26.
36 Streit M, Stephen AE, Hawighorst T *et al.* Systemic inhibition of tumor growth and angiogenesis by thrombospondin-2 using cell-based antiangiogenic gene therapy. *Cancer Res* 2002; **62**: 2004–12.
37 Leland PA, Raines RT. Cancer chemotherapy – ribonucleases to the rescue. *J Chem Biol* 2001; **8**: 405–13.
38 Leland PA, Staniszewski KE, Kim BM, Raines RT. Endowing human pancreatic ribonuclease with toxicity for cancer cells. *J Biol Chem* 2001; **276**: 43095–102.
39 Rybak SM, Newton DL. Natural and engineered cytotoxic ribonucleases: therapeutic potential. *Exp Cell Res* 1999; **253**: 325–35.
40 Futami J, Maeda T, Kitazoe M *et al.* Preparation of potent cytotoxic ribonucleases by cationization: enhanced cellular uptake and decreased interaction with ribonuclease inhibitor by chemical modification of carboxyl groups. *Biochemistry* 2001; **40**: 7518–24.
41 Folkman J. What is the evidence that tumors are angiogenesis dependent? *J Natl Cancer Inst* 1990; **82**: 4–6.
42 D'Amore PA, Shima DT. Tumor angiogenesis: a physiological process or genetically determined? *Cancer Metastasis Rev* 1996; **15**: 205–12.
43 Hori A, Sasada R, Matsutani E *et al.* Suppression of solid tumor growth by immunoneutralizing monoclonal antibody against human basic fibroblast growth factor. *Cancer Res* 1991; **51**: 6180–4.
44 Noguchi Y, Wu J, Duncan R *et al.* Early phase tumor accumulation of macromolecules: a great difference in clearance rate between tumor and normal tissues. *Jpn J Cancer Res* 1998; **89**: 307–14.
45 Dreher MR, Liu W, Michelich CR, Dewhirst MW, Yuan F, Chilkoti A. Tumor vascular permeability, accumulation, and penetration of macromolecular drug carriers. *J Natl Cancer Inst* 2006; **98**: 335–44.

doi: 10.1111/j.1349-7006.2006.00336.x

available at www.sciencedirect.com
journal homepage: www.europeanurology.com

European Association of Urology

From Lab to Clinic

p53 Protein Transduction Therapy: Successful Targeting and Inhibition of the Growth of the Bladder Cancer Cells

Miyabi Inoue [a], *Kazuhito Tomizawa* [b,*], *Masayuki Matsushita* [b], *Yun-Fei Lu* [b], *Teruhiko Yokoyama* [a], *Hiroyuki Yanai* [c], *Atsushi Takashima* [b], *Hiromi Kumon* [a], *Hideki Matsui* [b]

[a] *Department of Urology, Okayama University Graduate School of Medicine, Dentistry and Pharmaceutical Sciences, Okayama 700-8558, Japan*
[b] *Department of Physiology, Okayama University Graduate School of Medicine, Dentistry and Pharmaceutical Sciences, 2-5-1 Shikata-cho, Okayama 700-8558, Japan*
[c] *Department of Pathology, Okayama University Graduate School of Medicine, Dentistry and Pharmaceutical Sciences, Okayama 700-8558, Japan*

Article info

Article history:
Accepted August 23, 2005
Published online ahead of print on November 2, 2005

Keywords:
Gene therapy
Bladder epithelium
TAT
Adenovirus
Protein deliverly

Abstract

Introduction: Virus-mediated gene therapy for bladder cancer has some problems, such as efficiency of gene delivery and safety issues. We have reported that poly-arginine peptide (11R) has the ability to increase protein transduction in cells. Here, we show that p53 protein transduction using 11R is useful for targeting to bladder tumors and suppressing the growth of bladder cancer cells.

Materials and methods: An 11R-fused p53 protein (11R-p53) was transduced in bladder cancer cell lines (J82 and T24) to evaluate the anti-tumor effect. Cell viability was assessed by performing the 4-[3-(4-iodophenyl)-2-(4-nitrophenyl)-2H-5-tetrazolio]-1,3-benzene disulfonate (WST) assay. To investigate whether 11R-p53 enhanced the effect on anti-cancer drug-dependent apoptosis of bladder cancer cells, the cell lines were cotreated with 11R-p53 and cis-diaminedichloroplatinum (CDDP). Apoptotic cells were identified using Hoechst staining. To investigate the efficiency of protein transduction mediated by 11R in bladder tumors *in vivo*, SCID mice were transplanted with J82 cells in the bladder and 11R-GFP was transurethrally transduced into the bladder. The transduction of 11R-GFP in the tumor was examined by confocal microscopy.

Results: 11R-p53 inhibited the growth of both J82 and T24 cells in a dose-dependent manner. The transduction of 11R-p53 enhanced CDDP-dependent induction of apoptosis. Transurethral application of

* Corresponding author. Tel. +81 86 235 7107; Fax: +81 86 235 7111.
E-mail address: tomikt@md.okayama-u.ac.jp (K. Tomizawa).

0302-2838/$ – see front matter doi:10.1016/j.eururo.2005.08.019

11R-GFP resulted in transduction of GFP in bladder tumors but not in the normal bladder epithelium or subepithelial tissues.
Conclusion: The present results suggest that p53 protein transduction therapy may be a promising method for the treatment of bladder cancer.

1. Introduction

Mutations of the *p53* tumor suppressor gene are seen in as many as 40–50% of high grade transitional cell carcinomas (TCCs) in the bladder [1]. The mutations are associated with poor prognosis and with resistance to both chemotherapy and radiation therapy [1]. Bladder carcinoma would be an ideal target for *in situ* gene therapies, since intravesical therapy can be applied simply and reliably. Gene transfer by viral vectors takes advantage of the natural ability of viruses to enter cells and direct the expression of transgenes by the infected cells [2].

Although there have been several preclinical studies of gene transfer by adenovirus vector into TCC of the bladder [3,4], the efficiency of the adenoviral vector-mediated gene transfer is not sufficient for clinical trials [5]. Previous studies have shown the mechanisms accounting for the low efficiency of gene transfer in TCC [6–8]. Furthermore, previous studies have indicated that virus-mediated gene therapy has some safety issues, such as inflammatory response, viral toxicity and random integration of viral vector DNA into the host chromosomes [2].

The cellular delivery of various biological compounds such as bioactive proteins has recently been improved by conjugating the compounds to short peptides known as cell penetrating peptides (CPPs) [9]. Poly-arginine (6–12 residues) is one of the CPPs [10]. Eleven poly-arginine (11R)-fused p53 protein (11R-p53) effectively penetrates across the plasma membrane of oral cancer cells (>95% cells) and translocates into the nucleus [11]. The protein induces the activity of the p21/WAF1 promoter and inhibits the proliferation of human oral cancer cells, and its effect is equivalent to that of adenovirus-mediated p53 gene therapy [11]. It has been indicated that the protein transduction method has some advantages over viral vector-mediated gene transduction therapy in terms of safety, low toxicity and random integration of vector DNA [10].

In this study, we found that 11R-p53 was efficiently delivered into bladder cancer cell lines and inhibited the proliferation of the cells, and we investigated whether 11R-p53 enhanced the effect of CDDP, which is a standard anti-cancer drug for bladder cancer. Moreover, the transurethral application of protein transduction using 11R resulted in effective and specific expression of exogenous protein in the bladder tumor of a model mouse.

2. Materials and methods

2.1. Cell lines and cell culture

The human bladder cancer cell lines J82 and T24 were obtained from American Type Culture Collection. J82 was maintained in MEM medium (Invitrogen, Carlsbad, CA) supplemented with 10% fetal bovine serum, penicillin (100 U/ml) and streptomycin (100 U/ml). T24 was maintained in McCoy's 5A medium (Invitrogen) supplemented with 10% fetal bovine serum, penicillin (100 U/ml) and streptomycin (100 U/ml).

2.2. Production of 11R fusion proteins

Production of 11R-p53 and 11R-enhanced green fluorescent protein (11R-EGFP) was carried out as described previously [11].

2.3. Recombinant adenovirus preparation

The recombinant adenovirus (pAdex-p53) containing wild-type human p53 cDNA, chicken β-actin promoter and SV40 polyadenylation signal was produced using the Adenovirus Expression Vector Kit (Takara, Tokyo, Japan) as described previously [11].

2.4. Western blotting analysis and Immunocytochemistry

Western blot analysis for p53 was carried out at high stringency, essentially as described previously [12]. The blots were probed with a primary antibody against p53 (1:1000; Pab 1801, Santa Cruz Biotech. Inc., Santa Cruz, CA).

Immunocytochemistry was performed as described previously [11]. After immunostaining using anti-p53 antibodies, the cells were incubated with rhodamine phalloidin. The staining was observed using a confocal laser microscope (Fluoview™ FV300, Olympus).

2.5. Reporter assay for p53-driven transactivation

The reporter assay was performed as described previously [11].

2.6. Cell viability

Cell viability was assessed at each time point after infection by pAdex-p53 or the addition of 11R-p53 by measuring the conversion of the triazolium salt WST-1 to formazan according to the manufacturer's instructions (Roche Applied Science, Mannheim, Germany) as described previously [11].

2.7. Treatment of bladder cancer cells with cis-diaminedichloroplatinum (CDDP)

J82 and T24 cells cultured in 96-well multiplates were transfected with pAdex-p53 or transduced with 11R-p53. After 24 h, the cells were treated with 0.02 μg/ml CDDP (Amersham Pharmacia Biotech) for 4 h. The cells were then washed with PBS twice and new medium was added. The medium of the cells treated with 11R-p53 was replaced by fresh medium in the presence of 11R-p53 every 24 h. The cells were harvested 96 h after adding CDDP, and the WST-1 assay was performed to assess the cell growth.

2.8. Assay for CDDP-dependent apoptosis

J82 and T24 cells (~70% confluent) cultured on coverglasses in 24-well dishes were transfected with pAdex-p53 at an MOI of 20, or transduced with 11R-p53 (1 μM). After 24 h, the cells were treated with 0.2 μg/ml CDDP for 4 h. The cells were washed with PBS twice and were then placed in fresh medium. The cells were fixed with 4% paraformaldehyde (pH 7.4) for 36 h after adding the CDDP and the fixed cells were incubated with 3.3 μM Hoechst 33342 (Sigma-Aldrich Chemical) for 1 min. Fluorescent signals were observed with a fluorescence microscope and apoptotic cells were identified by the presence of highly condensed or fragmented nuclei. Representative graphs are shown for experiments in which at least 4 randomly chosen fields with 50 cells were scored.

2.9. Animal studies

The animal studies were approved by the Animal Research and Care Committee at Okayama University Graduate School of Medicine, Dentistry and Pharmaceutical Sciences. Female B6 severe combined immunodeficiency disease (SCID) ($H\text{-}2^b$) mice (8 weeks old) were purchased from CREA Japan (Tokyo, Japan). The mice were anesthetized with pentobarbital sodium (40 mg/kg i.p.) and were then injected in the bladder wall with 1×10^6 J82 cells suspended in PBS in a volume of 50 μl. Ten days later, at a time when the bladder tumors ulcerated the bladder mucosa, 200 μl of 11R-EGFP (10 μM) or EGFP (10 μM) proteins were transurethrally instilled into the bladder through polyethylene tubing PE90 (Instech Laboratories, Plymouth Meeting, PA) and the mice were sacrificed 6 hours after the protein transduction ($n = 8$ each group).

2.10. Hematoxylin and eosin (H-E) staining and immunohistochemistry

H-E staining and immunohistochemical analyses were done at high stringency essentially as described previously [13]. For immunohistochemistry, sections of the bladder were incubated with mouse monoclonal anti-human epidermal keratin (AE1/AE3) antibodies (1:100, PROGEN Biotechnik GmbH, Heidelberg, German) at 37 °C for 2 hours. After the antibodies were washed off, the sections were incubated with rhodamine-conjugated secondary antibodies (1:100). Fluorescent images were obtained using a laser confocal microscope with a 20 × lens.

2.11. Statistical analysis

Data are shown as the mean (±S.E.M.). Data were analyzed using either the Student's t-test to compare two conditions or ANOVA followed by planned comparisons of multiple conditions, and $p < 0.05$ was considered to be significant.

3. Results

3.1. The transduction and function of 11R-p53 in J82 and T24 cells

The J82 cell line expresses a p53 gene mutated in codons 271, 274, and 320, whereas the T24 cell line contains a *p53* allele encoding p53 with an in-frame deletion of tyrosine 126 [14]. To examine whether 11R-p53 protein was delivered into the bladder cancer cells through the plasma membrane, J82 and T24 cells were incubated with 1 μM 11R-p53. Time-dependent changes of the uptake of 11R-p53 in the cells were confirmed by Western blotting analysis. A high level of 11R-p53 was detected from 6 h to 24 h after the addition of the protein and the level was decreased after 12 h in J82 cells (Fig. 1A). After 48 h, the level of the transduced protein was low. 11R-p53 was also effectively transduced in T24 cells within 12 h. However, the protein was more rapidly degraded in these cells (Fig. 1A). The protein level was extremely low after 24 h.

To demonstrate whether 11R-p53 was localized in the nucleus of T24 cells, the cells were double-stained with anti-p53 antibody (green) and rhodamine phalloidin (red). p53 protein lacking 11R was not delivered in the cells whereas 11R-p53 was localized in nucleus of the cells (Fig. 1B). The transcription regulatory activity of 11R-p53 was also examined in J82 and T24 cells. Transduction of 11R-p53 resulted in high p53 transcription regulatory activity whereas p53 protein lacking 11R did not have the activity in the both cells (Fig. 1C).

3.2. Inhibitory effect of 11R-p53 on the growth of J82 and T24 cells

The dose-dependency of the inhibitory effect of 11R-p53 on the growth of J82 and T24 cells was next investigated. A low concentration (0.01 μM) of 11R-

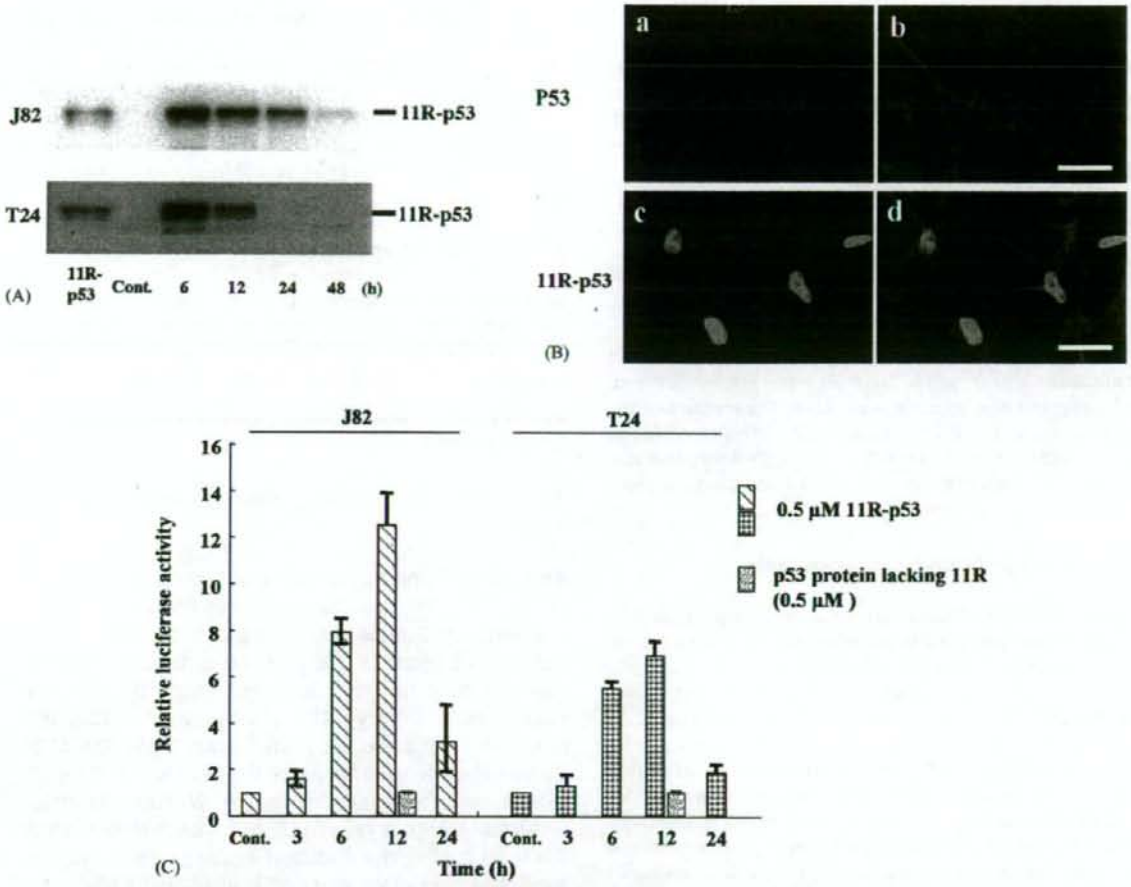

Fig. 1 – (A) Time-dependent changes of the level of transduced 11R-p53 in J82 and T24 cells. Purified 11R-p53 (0.1 μM) was added to the culture medium of each cell line. After 2 h, the cells were washed with PBS and were incubated in fresh medium in the absence of 11R-p53. The cells were further cultured and were harvested at each indicated time point after the addition of the protein. Western blot analysis was performed using anti-p53 antibodies. 11R-p53, 10 ng purified 11R-p53; Cont, no addition of 11R-p53. (B) The localization of p53 lacking 11R (p53) and 11R-p53 in T24 cells. a and c, 11R-p53 localization (green); b and c, Merged image with 11R-p53 (green) and F-actin (red). Bars, 50 μm. (C) Time-dependent changes of the transcription regulatory activity of 11R-p53 and p53 in J82 and T24 cells. A luciferase reporter vector carrying the p21/WAF1 promoter was transfected the cells. After 24 h, the cells were transduced with 11R-p53 or p53. As a control (Cont.), the cells were only transfected with the luciferase reporter vector. $n = 6$ in each group.

p53 had no effect on the growth of J82 cells (Fig. 2C). However, 0.1 μM 11R-p53 significantly inhibited the cell growth (Fig. 2C). Moreover, 0.5 μM and 1 μM 11R-p53 more severely inhibited the growth (Fig. 2A and C). The inhibitory effect of 0.5 μM 11R-p53 was the same as that of Adex-p53 at an multiplicity of infection (MOI) of 100 (Fig. 2C). The protein transduction of 11R-p53 had a small but statistically significant effect on the inhibition of the growth of T24 cells (Fig. 2B and D). However, the inhibitory effect on the growth of T24 cells was weaker than that on the growth of J82 cells (Fig. 2C and D). The inhibitory effect of pAdex-p53 was also weaker in T24 cells than in J82 cells (Fig. 2C and D).

3.3. *Co-treatment with 11R-p53 and CDDP enhances the anticancer effect of CDDP*

CDDP is one of the most widely used anticancer chemotherapeutic drugs for bladder cancer and

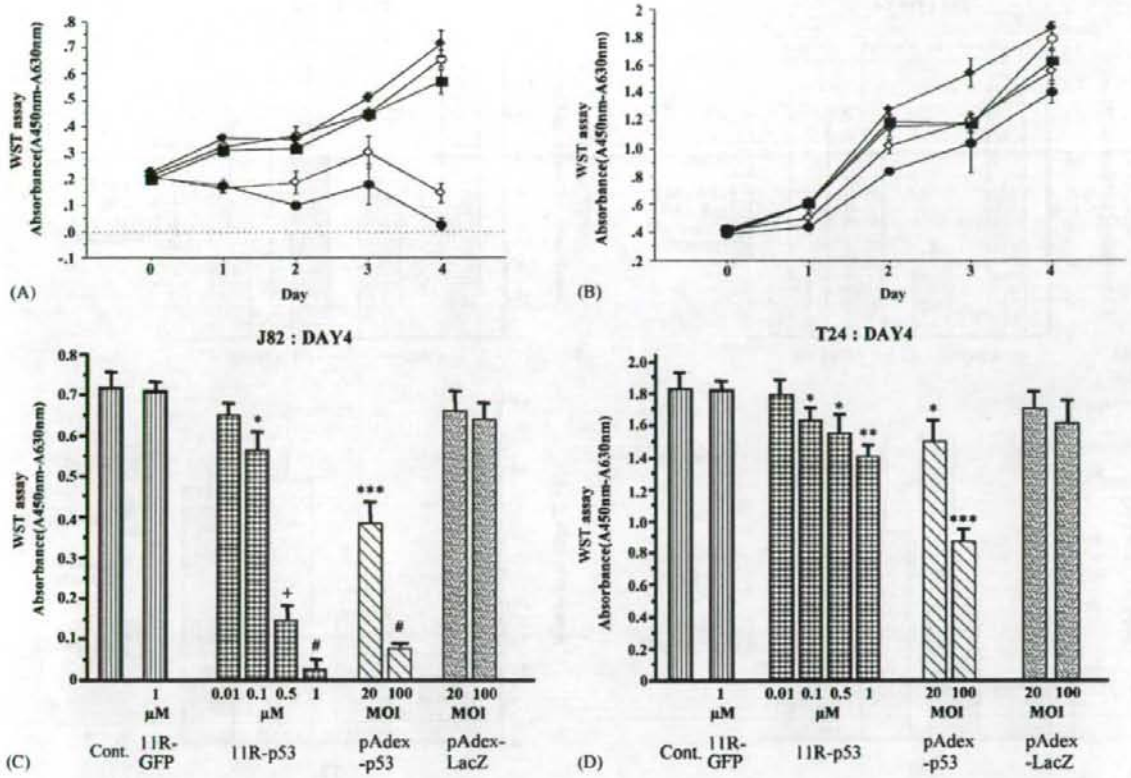

Fig. 2 – Effect of 11R-p53 and pAdex-p53 on the growth of J82 (A and C) and T24 (B and D) cells. A and B, Dose-dependent growth inhibition by 11R-p53. J82 and T24 cells were treated with each indicated concentration of 11R-p53 (◆, control; ✱, 0.01 μM; ■, 0.1 μM; ◇, 0.5 μM; ●, 1 μM 11R-p53) every 24 h. Cell growth was assessed every 24 h by the WST assay. C and D, Comparison of the inhibitory effects of 11R-p53, 11R-GFP and pAdex-p53. Each indicated concentration of 11R-p53 or 11R-GFP was applied every 24 h, while pAdex-p53 and -lacZ were transfected on Day 0. After 96 h, the cells were harvested and the WST assay was performed. $n = 6$ each, *, $p < 0.05$; **, $p < 0.01$; ***, $p < 0.001$; +, $p < 0.0005$ and #, $p < 0.0001$ compared with the control.

induces apoptosis of bladder cancer cells [15]. J82 and T24 cells were treated with 11R-p53 in combination with CDDP, and whether 11R-p53 enhanced the anti-cancer effect of CDDP was assessed by the WST assay. CDDP inhibited the growth of J82 and T24 cells (Fig. 3A and B). Co-treatment with 11R-p53 plus CDDP significantly enhanced the CDDP-dependent inhibition of the cell growth, and the enhancement by 11R-p53 was more potent than that by pAdex-p53 (Fig. 3A and B).

We next studied whether the protein transduction of 11R-p53 increased the CDDP-induced apoptosis of bladder cancer cells. J82 and T24 cells were treated with 11R-p53, CDDP or were co-treated with CDDP and 11R-p53 or pAdex-p53. The addition of 11R-p53 significantly enhanced the CDDP-dependent induction of the apoptosis of both cell lines to the same extent pAdex-p53 (Fig. 3C and D).

3.4. *Protein transduction in bladder tumors in vivo*

To test the efficiency of protein transduction using 11R in bladder tumors *in vivo*, SCID mice were transplanted with J82 cells in the bladder and were transurethrally administered 10 μM 11R-GFP (200 μl) or GFP (200 μl). The histological features of the bladder tumors were confirmed with H-E staining (Fig. 4E), and the tumor tissue was visualized with immunofluorescent staining of human epidermal keratin (Fig. 4A). Interestingly, 11R-GFP was colocalized with the keratin staining (Fig. 4B and D). There was little transduction of 11R-p53 in normal bladder epithelium or the subepithelial tissues such as bladder smooth muscle (Fig. 4B, C and D). Transurethral application of GFP without 11R failed to transduce the protein in the bladder tumors or the normal bladder (data not shown).

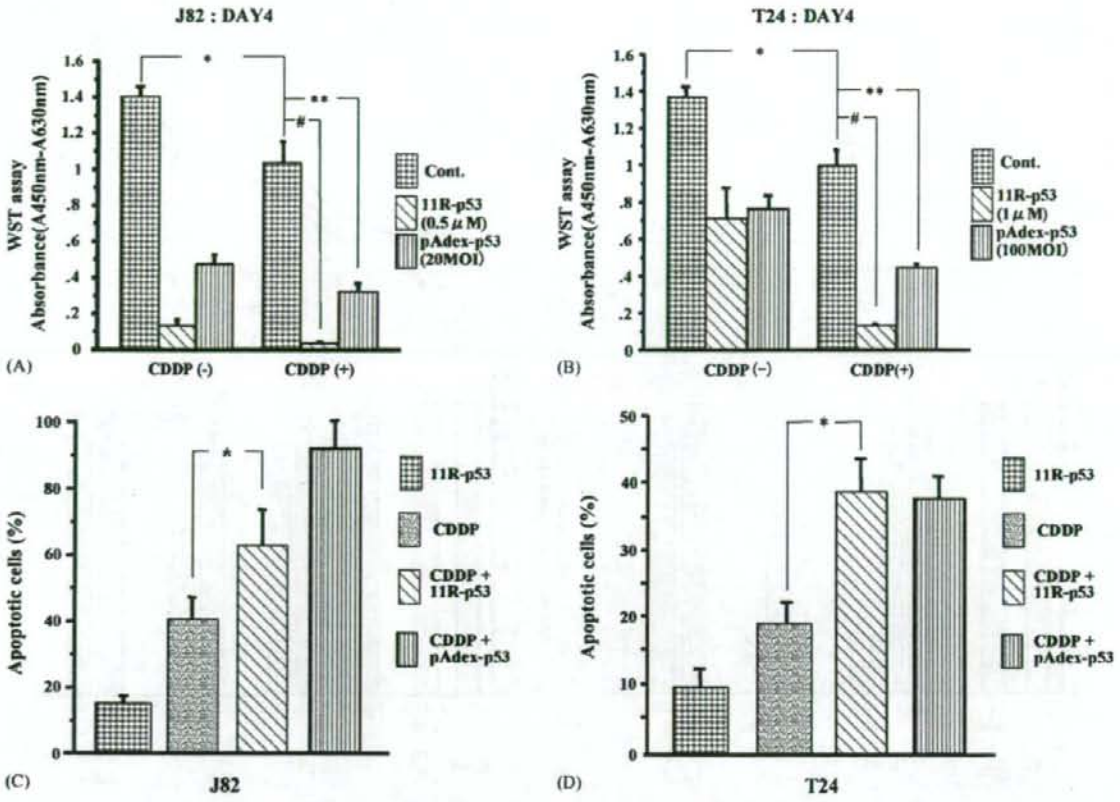

Fig. 3 – Synergistic effects of 11R-p53 in combination with CDDP on the inhibition of growth (A and B) and induction of apoptosis (C and D) of J82 and T24 cells. A and B, Cell viability after each treatment was assessed using the WST assay 96 h after adding CDDP. $n = 6$ each, *, $p < 0.05$; **, $p < 0.01$ and #, $p < 0.001$. C and D, The cells were treated with 11R-p53, CDDP or were co-treated with CDDP and 11R-p53 or pAdex-p53. After Hoechst staining, fluorescent signals were observed with a fluorescence microscope and apoptotic cells were identified by the presence of highly condensed or fragmented nuclei. $n = 50$ in each treatment. *, $p < 0.01$.

4. Discussion

Intravesical administration of Bacillus Calmette-Guerin (BCG) after transurethral resection is the most effective treatment for the high grade superficial bladder TCC [16]. However, approximately one-third of patients with pT1G3 tumors fail to respond to BCG therapy [17]. Mutations of the *p53* gene are correlated with the clinical response to intravesical BCG therapy [17]. Bladder tumors expressing a mutant *p53* gene are resistant to BCG therapy [17]. Thus, the development of novel therapeutics for the treatment of patients with pT1G3 tumors expressing a mutant *p53* gene is required. It has been expected that viral vector-mediated delivery of the *p53* gene would be a powerful strategy for high grade superficial bladder TCC. However, the efficiency of the virus-mediated gene delivery is limited in bladder tumors [6–8]. In the present study, a protein transduction method using 11R effectively delivered p53 protein into bladder cancer cells and inhibited the growth of the cells. These results suggest that 11R-p53 transduction therapy may become an attractive approach for the treatment of BCG-resistant bladder cancer with p53 mutations.

One of the most interesting findings in the present study is that transurethral protein transduction using 11R selectively delivered proteins into bladder tumors and the delivered proteins were transduced not only in the surface but also in the center of the tumor. The present results showed that 11R-p53 in combination with CDDP significantly inhibited the growth of bladder cancer cells expressing a mutant *p53* gene. These results suggest that 11R-p53 protein transduction in combination with intravenous CDDP may become a therapy option for high grade invasive bladder tumors with a mutant *p53* gene.

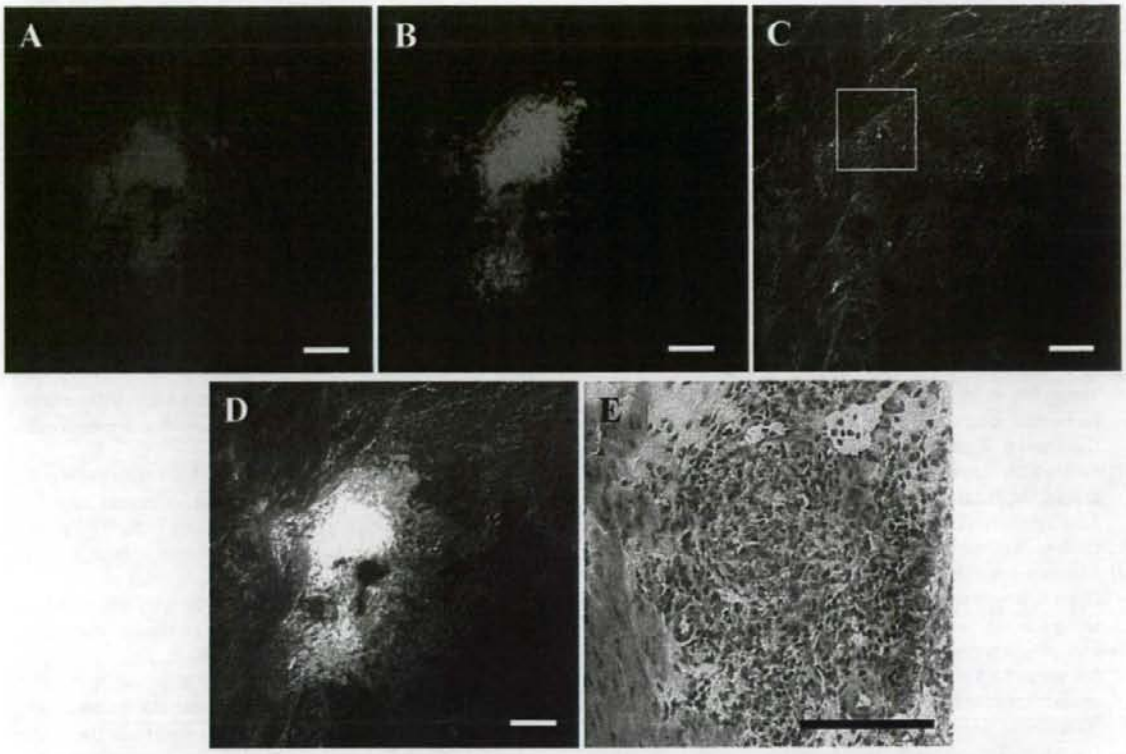

Fig. 4 – Protein transduction of 11R-GFP in bladder tumors *in vivo*. SCID mice were transplanted with J82 cells in the bladder. After 10 days, 11R-GFP was transurethrally transduced in the bladder. A, Immunohistochemical analysis of human epidermal keratin in the tumor-transplanted bladder. B, The expression of 11R-GFP in the bladder. C, Bright field image of the same area. D, Merged image of human epidermal keratin (red) and 11R-GFP (green). Colocalization of human epidermal keratin and 11R-GFP was observed. E, H-E staining in the boxed area in C. H-E staining revealed that the localization of the strong expression of 11R-GFP was colocalized with the tumor formation of J82 cells in SCID mice. Scale bars = 100 μm.

An ideal therapeutic agent for cancer would be one that could be systemically delivered, and that would selectively target tumor cells and be nontoxic to normal cells. The present results suggest that the protein transduction method is a promising system for tumor-targeted p53 protein delivery that may have potential for the treatment of bladder tumor. The anti-tumor effect of transurethral 11R-p53 protein transduction on bladder tumors in a mouse model is currently under investigation in our laboratory.

5. Conclusions

11R-p53 was effectively delivered into bladder cancer cells and significantly inhibited the growth of the cells. Moreover, 11R-p53 enhanced the CDDP-dependent induction of apoptosis of the cells. Transurethral application of protein transduction using 11R effectively and selectively delivered exogenous protein into bladder tumors *in vivo*. These results suggest that p53 protein transduction therapy may become a novel method for bladder cancer therapy.

Acknowledgement

This work was supported by a Grant-in-Aid for Scientific Research from the Ministry of Education, Science, Sports and Culture of Japan.

References

[1] Al-Sukhun S, Hussain M. Current understanding of the biology of advanced bladder cancer. Cancer 2003;8:2064–75.

[2] Verma IM, Somia N. Gene therapy-promised, problems and prospects. Nature 1997;389:239–42.
[3] Werthman PE, Drazan KE, Rosenthal JT, Khalili R, Shaked A. Adenoviral-p53 gene transfer to orthotopic and peritoneal murine bladder cancer. J Urol 1996;155:753–6.
[4] Chester JD, Kennedy W, Hall GD, Selby PJ, Knowles MA. Adenovirus-mediated gene therapy for bladder cancer: efficient gene delivery to normal and malignant human urothelial cells in vitro and ex vivo. Gene Ther 2003; 10:172–9.
[5] Siemens DR, Crist S, Austin JC, Tartaglia J, Ratliff TL. Comparison of viral vectors: gene transfer efficiency and tissue specificity in a bladder cancer model. J Urol 2003;170:979–84.
[6] Li Y, Pong RC, Bergelson JM, Hall MC, Sagalowsky AI, Tseng CP, et al. Loss of adenoviral receptor expression in human bladder cancer cells: a potential impact on theefficacy of gene therapy. Cancer Res 1999;59:325–30.
[7] Sachs MD, Rauen KA, Ramamurthy M, Dodson JL, De Marzo AM, Putzi MJ, et al. Integrin alpha (v) and coxsackie adenovirus receptor expression in clinical bladder cancer. Urology 2002;60:531–6.
[8] Watanabe T, Shinohara N, Sazawa A, Harabayashi T, Ogiso Y, Koyanagi T, et al. An improved intravesical model using human bladder cancer cell lines to optimize gene and other therapies. Cancer Gene Ther 2000;7:1575–80.
[9] Schwarze SR, Hruska KA, Dowdy SF. Protein transduction: unrestricted delivery into all cells? Trends in Cell Biol 2000;10:290–5.
[10] Matsui H, Tomizawa K, Lu YF. Protein Therapy: in vivo protein transduction by polyarginine (11R) PTD and subcellular targeting delivery. Curr Protein Pept Sci 2003; 4:151–7.
[11] Takenobu T, Tomizawa K, Matsushita M, Li ST, Moriwaki A, Lu YF, et al. Development of p53 protein transduction therapy using membrane-permeable peptides and the application to oral cancer cells. Mol Cancer Ther 2002; 1:1043–9.
[12] Tomizawa K, Iga N, Lu YF, Moriwaki A, Matsushita M, Li ST, et al. Oxytocin improves long-lasting spatial memory during motherhood through MAP kinase cascade. Nat Neurosci 2003;6:384–90.
[13] Nozaki K, Tomizawa K, Yokoyama T, Kumon H, Matsui H. Calcineurin mediates bladder smooth muscle hypertrophy after bladder outlet obstruction. J Urol 2003;170:2077–81.
[14] Cooper MJ, Haluschak JJ, Johnson D, Schwartz S, Morrison LJ, Lippa M, et al. p53 Mutations in bladder carcinoma cell lines. Oncol Res 1994;6:569–79.
[15] Mizutani Y, Nakao M, Ogawa O, Yoshida O, Bonavida B, Miki T. Enhanced sensitivity of bladder cancer cells to tumor necrosis factor related apoptosis inducing ligand mediated apoptosis by cisplatin and carboplatin. J Urol 2001;165:263–70.
[16] Herr HW, Wartinger DD, Fair WR, Oettgen HF. Bacillus Calmette-Guerin therapy for superficial bladder cancer: a 10 year followup. J Urol 1992;147:1020–3.
[17] Pfister C, Flaman JM, Dunet F, Grise P, Frebourg T. p53 mutations in bladder tumors inactivate the transactivation of the p21 and Bax genes, and have a predictive value for the clinical outcome after bacillus Calmette-Guerin therapy. J Urol 1999;162:69–73.

Chem Biol Drug Des 2006; **67:** 238–243

Research Article

doi: 10.1111/j.1747-0285.2006.00360.x

A Cell-permeable NFAT Inhibitor Peptide Prevents Pressure-Overload Cardiac Hypertrophy

Mitsuhito Kuriyama[1,2], Masayuki Matsushita[1,*], Atsushi Tateishi[2], Akiyoshi Moriwaki[1], Kazuhito Tomizawa[1], Kozo Ishino[2], Shunji Sano[2] and Hideki Matsui[1]

[1]Department of Physiology, Okayama University Graduate School of Medicine and Dentistry, 2-5-1 Shikata-cho, Okayama 700-8558, Japan

[2]Department of Cardio-Vascular Surgery, Okayama University Graduate School of Medicine and Dentistry, 2-5-1 Shikata-cho, Okayama 700-8558, Japan

**Corresponding author: Masayuki Matsushita, Tel: (+81) 42-724-6290, Fax: (+81) 42-724-6316, masayuki@libra.ls.m-kagaku.co.jp*

The activation of the calcineurin–nuclear factor of activated T cells cascade during the development of pressure-overload cardiac hypertrophy has been previously reported in a number of studies. In addition, numerous pharmacological studies involving calcineurin inhibitors such as FK506 and cyclosporine A have now demonstrated that these agents can prevent such hypertrophic responses in the heart. However, little is known regarding the roles of the calcineurin downstream effecter – nuclear factor of activated T cells. Our present study has further examined the roles of nuclear factor of activated T cells in pressure-overload cardiac hypertrophy by employing a recently developed cell-permeable nuclear factor of activated T cells inhibitor peptide. Rat hearts were subjected to pressure overload attributable by 4 weeks of aortic banding, and then treated with this cell-permeable nuclear factor of activated T cells inhibitor peptide and a control peptide. Treatment with the inhibitor was found to significantly decrease the heart weight/body weight ratio, the size of cardiac myocytes, and the serum brain natriuretic peptide and atrial natriuretic peptide levels. These results suggest that nuclear factor of activated T cells functions in a key role in the development of cardiac hypertrophy during pressure overload. Inhibition of nuclear factor of activated T cells by a specific inhibitor peptide is a suitable method for characterization of the molecular mechanisms underlying cardiac hypertrophy as well as in the search for new promising therapies for disease.

Key words: cardiac hypertrophy, calcineurin, NFAT, protein transduction

Received 20 October 2005, revised 20 January 2006 and accepted for publication 4 February 2006

Cardiac hypertrophy can be observed in various cardiovascular diseases, including hypertension, mechanical load, myocardial infarction, endocrine disorders and genetic mutations in cardiac proteins (1,2). Hypertrophic stimulation also triggers numerous intracellular signaling pathways, such as those of the mitogen-activated protein kinases (MAPKs), Ca^{2+}/calmodulin-dependent protein kinases (CaMKs), protein kinase C (PKC), PI3K and Ca^{2+}/calmodulin-dependent protein phosphatase (calcineurin) (3,4). Many pharmacological studies involving calcineurin (CaN) inhibitors such as FK506 and cyclosporine A (CysA) now have demonstrated a critical function for CaN in the hypertrophic response, which links alterations in intracellular calcium handling in heart myocytes to this process (5–7). The roles of the CaN downstream transcriptional effecter, nuclear factor of activated T cells (NFAT), in cardiac hypertrophy have also been previously documented (8). During transplantation, the immunosuppressants CysA and FK506, which are used clinically to prevent organ rejection, inhibit CaN phosphatase activity towards all of its protein substrates, including NFAT (9,10). Although these drugs have revolutionized transplant therapy, their persistent use can now be associated with a progressive loss of renal function, hypertension, hyperglycemia, neurotoxicity and an increased risk of malignancy (11,12).

Recently, a NFAT inhibitor peptide (VIVIT) was developed based on the conserved CaN docking site within the NFAT family members (13). This peptide interferes selectively with the CaN–NFAT interaction without affecting CaN phosphatase activity.

Expression of green fluorescent protein (GFP)-VIVIT in myocytes inhibited the NFAT activation *in vitro* was demonstrated (14). Therefore, the NFAT inhibitor peptide may be beneficial as a therapeutic agent characterized by reduced toxicity in comparison to current drugs. We synthesized the cell-permeable NFAT inhibitor peptide via a poly-arginine-based protein transduction system (*11R*) (15). Protein transduction systems have been developed for the delivery of bioactive peptides and proteins into eukaryotic cells *in vitro* and *in vivo* (16,17). These protein delivery systems have been proved useful with respect to providing answers to important biological questions (16–18).

In our present study, this synthetic NFAT inhibitor peptide was employed to elucidate the various roles of NFAT in pressure-overload cardiac hypertrophy and to characterize its therapeutic potential to prevent the development of this disorder. Our subsequent findings in rats have revealed that this specific NFAT inhibitor peptide prevents increased heart weight and serum concentrations of brain natriuretic peptide (BNP) and atrial natriuretic peptide (ANP) during the pressure-overload hypertrophic response.

Methods and Materials

Peptide sequence and synthesis

Peptides described in this report include the following: **11R-VIVIT** (H-Arg-Arg-Arg-Arg-Arg-Arg-Arg-Arg-Arg-Arg-Gly-Gly-Gly-Met-Ala-Gly-Pro-His-Pro-Val-Ile-Val-Ile-Thr-Gly-Pro-His-Glu-Glu-NH_2); **11R-VEET** (H-Arg-Arg-Arg-Arg-Arg-Arg-Arg-Arg-Arg-Arg-Arg-Arg-Gly-Gly-Gly-Met-Ala-Gly-Pro-Pro-His-Ile-Val-Glu-Glu-Thr-Gly-Pro-His-Val-Ile-NH_2); and **VIVIT** (H-Met-Ala-Gly-Pro-His-Pro-Val-Ile-Val-Ile-Thr-Gly-Pro-His-Glu-Glu-NH_2). All peptides were synthesized according to the Fmoc (9-fluorenylmethoxycarbonyl) strategy using a PSSM-8 peptide synthesizer (Shimadzu, Japan). Labeling of the N-termini of the peptides with the NHS-Fluorescein [5-(and 6)-carboxyfluorescein, succinimydyl ester] probe was performed as follows: Resin-bound peptides were treated with piperidine [30% (v/v) in dimethylformamide (DMF)] to remove the N-terminal Fmoc protecting group. NHS-Fluorescein was added in dry DMF (10-fold molar excess) for 12 h in the dark to selectively label the N-terminal amino group. The resin was then washed with DMF and treated with a deprotecting mixture to cleave the peptides from the resin and deprotect the side-chains. Peptide purification was carried out by RP-HPLC (TOSOH, Japan) using a trifluoroacetic acid 0.1%/acetonitrile gradient. The purity as assessed by reversed-phase liquid chromatography (Beckman Gold equipped with a Diode Array detector; Thermo Electron Corporation, Madison, WI, USA) was over 95% for each peptide using the criterion of the relative UV absorbance at 214 nm. The molecular masses were validated by electrospray ionization mass spectrometry (Thermo Electron Corporation). These peptides were found to be identical to those previously described (15).

Animal model of pressure overload

Male Wistar rats (8 weeks old; 250–270 g) were obtained from Shimizu (Japan) and were divided into five groups: normal rats, pressure overload rats, pressure overload rats with CysA, pressure overload rats with 11R-VIVIT and pressure overload rats with 11R-VEET ($n = 6$ for each group). Pressure overload was produced by constriction of the abdominal aorta. Animals were anesthetized via a sodium pentobarbital injection (50 mg/kg i.p.) and a laparotomy was subsequently performed to expose the abdominal aorta. The abdominal aorta was then constricted above the right renal artery with a 6–0 proline which was tied around both the aorta and a blunted 24-gauge polyethylene catheter. The catheter was eventually removed. The abdomen was closed with 3–0 silk following antibiotic prophylaxis with procaine penicillin G (10 000 U). Subcutaneous injections (SC) of CysA at 20 mg/kg/2 days SC, 11R-VIVIT at 10 mg/kg/2 days SC, or 11R-VEET at 10 mg/kg/2 days were administered from one day after the pressure overload procedure throughout a 4-week period.

Echocardiographic analysis

At 27 days following surgery, transthoracic echocardiographic analysis was performed with the Power Vision8000 (SSA-390A, Toshiba Co., Tokyo, Japan) with a 7.5-MHz imaging transducer for the heart and an 11-MHz imaging transducer for the abdominal aorta. Rats were anesthetized via sodium pentobarbital injection (50 mg/kg i.p.) and subsequently, M-mode images of the LV and abdominal aorta were subsequently recorded as described previously.

Histological analysis

Hearts were cut into 30-μm sections with a freezing microtome following fixation with Zamboni's fixative. The sections were then counterstained with hematoxylin-eosin or were directly examined by confocal microscopy.

Western blot analysis

Detection of CaN by immunoblotting was conducted with CaN antibody (Santa Cruz) and actin (Sigma) antibodies in 5% milk powder in TBS, containing 0.1% Tween-20, for 2 h at room temperature. Detection was then performed using enhanced chemiluminescence (Amersham Pharmacia, Princeton, NJ, USA). CaN and Actin bands were quantified by densitometry using NIH IMAGE software. Samples from both the control and pressure-overloaded rat hearts were analyzed on individual immunoblots. For each experiment, the values obtained for the treated hearts were calculated relative to the values obtained for the control slices. Normalized data from five experiments were averaged, and statistical analysis was carried out by using one-way ANOVA.

Toxicity levels of the 11R-VIVIT peptide

Serum levels of glutamate oxaloacetate transaminase (GOT), glutamate pyruvate transaminase (GPT), creatinine phosphokinase (CPK), alkaline phosphatase, blood urea nitrogen (BUN) and creatinine (Cr) were measured by SRL Inc., Japan.

Statistics

All values were expressed as the mean ± SEM of six experiments in each instance. Comparisons of two groups were performed via the paired *t*-test (SSPE). Statistical significance was at $p < 0.05$.

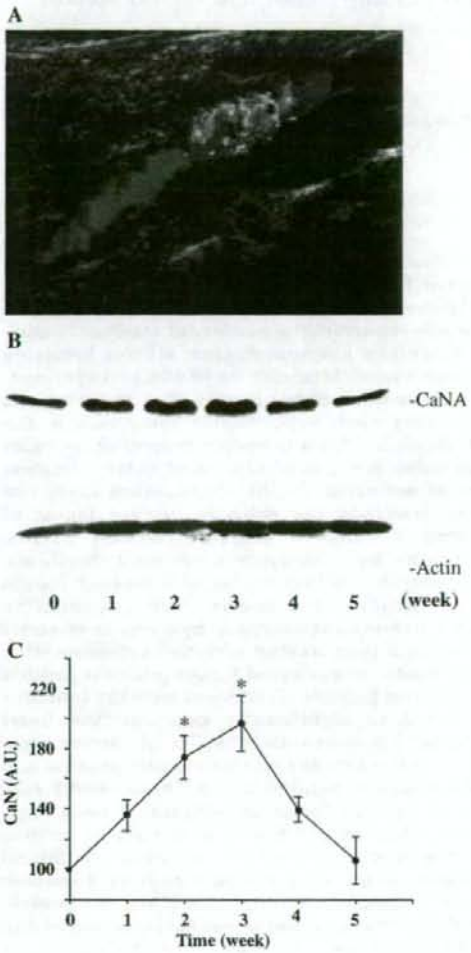

Figure 1: CaN protein levels are increased in a pressure-overload rat model. (A) Representative example of a color UCG image showing an aorta banding signal in a rat model. (B) Representative expression of CaN-A in rat heart tissue during pressure-overload cardiac hypertrophy. For immunodetection analysis, 10 μg of total protein was applied to each lane, and CaN-A-specific and β-actin antibodies were utilized for detection. (C) Data are represented as mean ± SEM of five animals. *$P < 0.05$; compared with week 0.

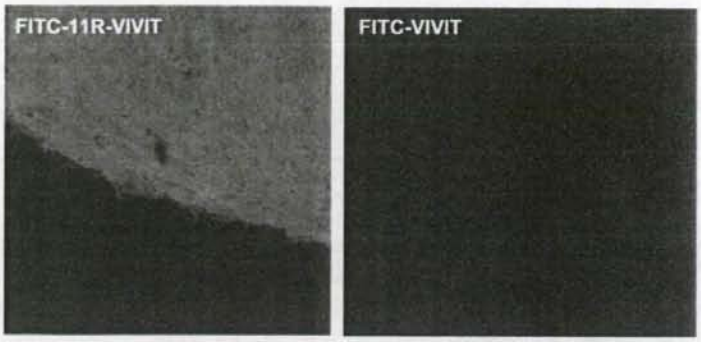

Figure 2: Successful delivery of FITC-11R-VIVIT into rat heart. Examination of FITC-11R-VIVIT and FITC-VIVIT localization in the rat heart after IP administration.

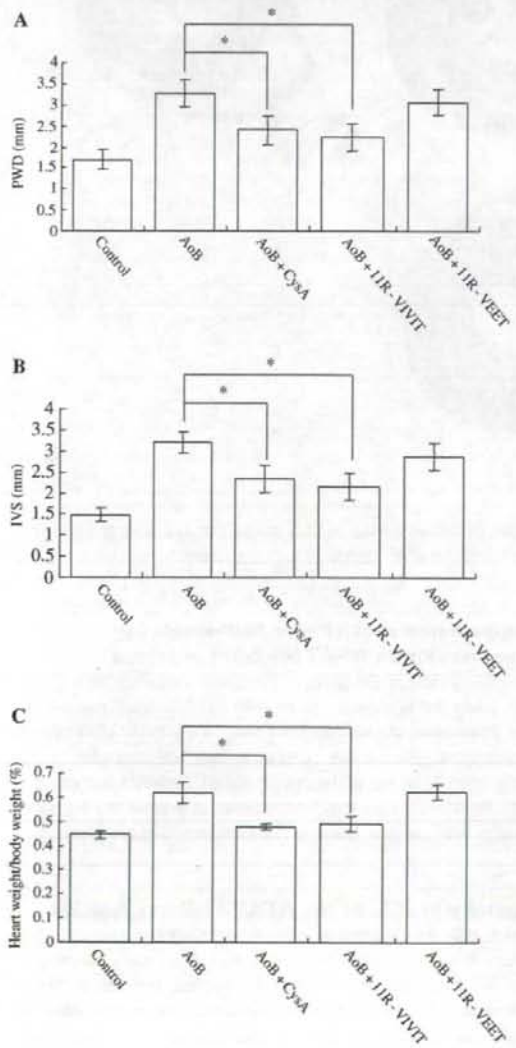

Results

Expression profiles of calcineurin

A rat model characterized by the constriction of the abdominal aorta was generated in order to examine the roles of NFAT in pressure-overload hypertrophy (Figure 1A). Previous studies had demonstrated an elevated CaN activity during pressure-overload cardiac hypertrophy. The expression levels of the CaN-A subunit in our rat model were evaluated by immunoblotting and were found to have increased over 3 weeks and decreased to the basal levels after 5 weeks (Figures 1B and C). Moreover, these expression levels positively correlated with the extent of the hypertrophic reaction in the rat hearts. A further examination of the subject animals via UCG revealed that the maximum levels of cardiac hypertrophy were reached at 3 weeks after the induced abdominal aortic contraction.

Delivery of the FITC-11R-VIVIT peptide to the rat heart

To examine whether 11R-VIVIT could be transduced into the rat heart, the animals were separately treated with FITC-conjugated 11R-VIVIT and VIVIT that had both been FITC-conjugated at the N-terminus. Four hours after the transduction, the presence of these two peptides in the heart was investigated by confocal microscopy (Figure 2). A strong FITC-11R-VIVIT signal could be observed, but in contrast, no FITC-VIVIT signal was detectable (Figure 2).

NFAT inhibitor peptide prevents pressure-overload cardiac hypertrophy in rats

Pressure overload was applied for 4 weeks in rat hearts and induced a marked cardiac hypertrophy. Chronic treatment with CysA and 11R-VIVIT, however, was found to prevent the development of the associated cardiac hypertrophy (Figure 3). Significant differences

Figure 3: Suppression of cardiac dimensions by NFAT inhibitor. Quantification by echocardiography (six), following aorta banding over 4 weeks, during which 11R-VIVIT and CysA were administered, demonstrates significant attenuation of PWD (A), IVS (B) and heart weight/body weight (C). Data are represented as mean ± SEM of six animals. *$p < 0.05$; compared with the control.

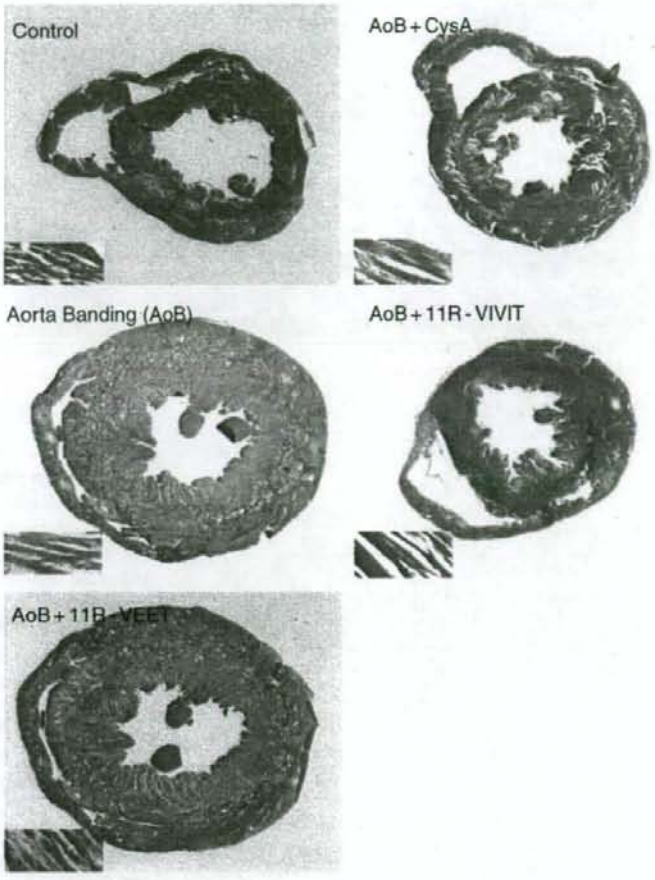

Figure 4: Gross morphologies of the histological cross-sections of rat hearts from the indicated groups. Aortic banding induced a noticeable hypertrophic response (A), which was abolished by 11R-VIVIT and CysA treatment. Treatment with a control peptide (11R-VEET) treatment did not prevent the hypertrophic response.

in body weight were not observed among the five groups but the application of pressure overload for 4 weeks markedly increased the ratio of heart weight to body weight (banded group, 62 ± 4.3% versus control, 44.5 ± 1.6%) (Figure 3C). Significantly, the administration of CysA and 11R-VIVIT prevented a pressure overload increase in the ratio of heart weight to body weight (banded group with CysA, 48 ± 1.2%, banded group with 11R-VIVIT, 49.2 ± 3.3%) (Figure 3C). Echocardiographic analysis further revealed that pressure overload increases the thickness of both the interventricular septum (IVS) (banded, 3.2 ± 0.25 mm versus control, 1.49 ± 0.16 mm) and the thickness of LV posterior wall (PW) (banded, 3.28 ± 0.33 mm versus control, 1.71 ± 0.23 mm) (Figures 3A and B). Treatment with CysA and 11R-VIVIT, however, inhibited this incremental wall thickening without affecting cardiac function (treated with CysA: IVS, 2.34 ± 0.32 mm, PW, 2.4 ± 0.35 mm, treated with 11R-VIVIT: IVS, 2.16 ± 0.32 mm, PW, 2.23 ± 0.32 mm) (Figures 3A and B).

Histological analysis

Histological analysis of the left ventricular cardiac tissue in our subject rats was performed to examine myocyte organization (Figure 4). Upon gross inspection, hematoxylin- and eosin-stained sections appeared normal for the banded groups that had been treated with CysA and 11R-VIVIT, compared with the control.

Suppression of ANP and BNP levels by treatment with NFAT inhibitor peptides

An induced state of the pressure overload in rat hearts for a period of 4 weeks led to elevated serum ANP and BNP levels (Figures 5A and B). However, chronic treatment with CysA and 11R-VIVIT caused a striking reduction in the increase in both ANP and BNP in our aortic banding rat model (Figures 5A and B). Furthermore, treatment with the 11R-VEET control peptide failed to prevent the enhancement of ANP and BNP levels in this experiment (Figures 5A and B).

Toxicity profile of the NFAT inhibitor peptide

Serum BUN and creatinine levels were indistinct among the five groups of rats that we tested in this study. Additionally, serum GOT and GPT levels also did not differ among these five groups. Moreover, serum CPK was not elevated in any of the groups (Table 1). Based upon electrocardiogram analysis, arrhythmia, e.g., A-V block,

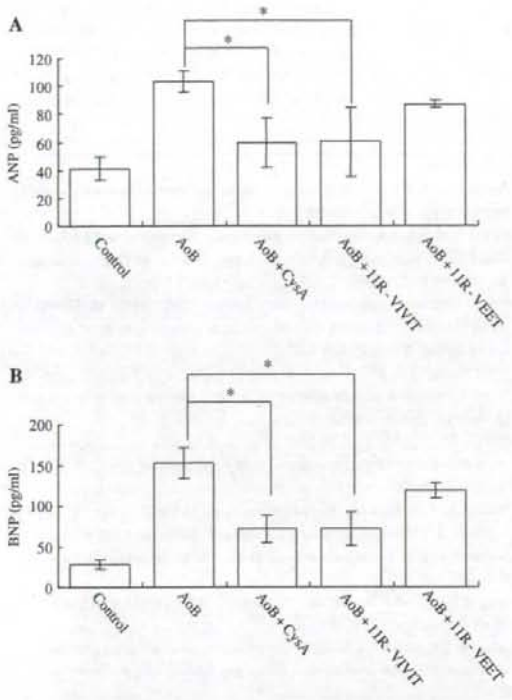

Figure 5: Examination of serum ANP and BNP levels following treatment with NFAT inhibitors. Aortic banding induced noticeable serum ANP (A) and BNP responses (B), which were significantly reduced by 11R-VIVIT and CysA treatments. Control peptide (11R-VEET) treatment, however, did not attenuate these ANP and BNP responses (A and B). Data are represented as mean ± SEM of six animals. *$p < 0.05$; compared with the control.

Table 1: Assessment of plasma levels of GOT, GPT, BUN, Cr (mean ± SEM) f weeks post-AoB

	Control	AoB	AoB/CysA	AoB/ 11R-VIVIT	AoB/ 11R-VEET
GOT (IU)	81.2 ± 4.35	94.2 ± 14.9	114 ± 23.6	99.2 ± 6.24	82.1 ± 7.34
GPT (IU)	49.6 ± 2.42	63.1 ± 14.6	52.2 ± 6.28	55.8 ± 9.95	60.5 ± 8.73[a]
BUN(mg/dl)	16.3 ± 1.13	21.5 ± 1.38	16.9 ± 1.48	16.6 ± 2.71	18.4 ± 1.82
Cr (mg/dl)	0.27 ± 0.02	0.37 ± 0.03	0.28 ± 0.04	0.28 ± 0.02	0.33 ± 0.03

[a]The differences between these levels and the control group are statistically significant ($p < 0.05$).

SPC and VPC, was also not detected (data not shown). These data strongly suggest the absence of any toxicity associated with the NFAT inhibitor peptide at the dose of 10 mg/kg used in these analyses.

Discussion

As a result of numerous investigations involving cell and animal models, a diverse number of signaling molecules have been implicated in the stimulus–response pathway by which the hypertrophic growth of the myocardium is controlled (2–4). Previously, CaN was subjected to extensive analysis due to its ability to regulate cardiac hypertrophy in a positive manner in culture, in both animal models and in human (3,4). Moreover, these studies also demonstrated the existence of a link between pressure-overload cardiac hypertrophy and the CaN-NFAT cascade. In our current study, an NFAT inhibitor peptide was generated, in further evaluate the role of NFAT as a regulator of the cardiac hypertrophic response *in vivo*.

In cardiac hypertrophy, the immunosuppressants CysA and FK506, used experimentally to prevent the progression of this disorder, inhibit the activity of CaN towards all of its protein substrates, including NFAT and prevent the NFAT nuclear import. In addition, activated CaN is necessary to maintain the transcriptional activity of NFAT, not by promoting its import but by suppressing its export (19). The suppression of the NFAT nuclear export process via CaN binding is also a prerequisite to the formation of effective NFAT transcriptional complexes (20). In this regard, the inhibition of CaN/NFAT binding may prove to be a more effective way of preventing the cardiac hypertrophy. To inhibit the CaN/NFAT binding, we employed the cell permeable VIVIT peptide. In recent years, based on these initial protein transduction domain (PTD) sequences, a PTD was developed that is characterized by an enhanced efficiency and a higher transduction rate. In particular, PTDs containing 6–11 arginine residues have garnered much attention due to their higher transduction rate and fewer side effects (21). Hence, we utilized the 11 arginine PTD peptide for the delivery of VIVIT peptide into the heart muscle cells of rat.

The principal objective of our current investigation was then to determine whether an NFAT-specific inhibitor peptide can block the CaN–NFAT signal cascade in the presence of pressure-overload left ventricular hypertrophy in rats. We subsequently found that aorta banding rats treated with 11R-VIVIT and CysA exhibited a significant reduction in their level of cardiac hypertrophy (Figures 3 and 5). In addition, this inhibitory peptide also reduced the BNP and ANP levels (Figure 5). However, we could not show whether these effects were due to the prevention of hypertrophy or caused by the direct inhibition of the BNP promoter, which is regulated by NFAT (8). The vast majority of the previous studies in this area have employed FK506 or CysA to prevent pressure-overload cardiac hypertrophy. Our current results indicate that the delivery of NFAT inhibitor peptide *in vivo* is an effective treatment for this disorder. It is noteworthy also that a fused peptide, utilized at the cell culture level, can also be delivered into various organisms *in vivo*, which is a considerable advantage of the PTD-related methodologies.

Concluding Remarks and Future Directions

A cell-permeable NFAT inhibitor peptide prevents the development of pressure-overload cardiac hypertrophy in a rat model. We demonstrate that the intracellular delivery of biologically active peptides by poly-arginine-mediated transduction can modify specific pathways *in vivo* and that this approach offers potential in terms of the production of novel classes of therapeutic peptides.

Although therapeutic agents that are based upon peptide-based strategies are promising, the half-life of such peptide molecules *in vivo* may remain problematic. High peptide doses were administered in our present study for treatment of the rats. An approach using retro-inverso peptide analogs derived from D-isomer amino acid residues may resolve the stability problem (22). Specifically using this method, retro-inverse TAT-p53 c terminal peptide treatment of cancer models has been previously shown to result in a significant increase in lifespan and in the generation of disease-free animals. Another chemical strategy, referred to as hydrocarbon stapling, for the production of BH3 peptides, referred to as hydrocarbon stapling, has also resulted in improved pharmacologic properties of peptide agents (23). Such stapled peptides proved to be helical, protease-resistant and cell-permeable molecules having increased affinity to multi-domain BCL-2 member pockets. Overall, these novel strategies may, therefore, have the potential to greatly enhance the pharmacological effectiveness of peptide-based therapeutic strategies.

Acknowledgments

This work was supported by a Grant-in-Aid for Scientific Research on Priority Areas (C) "medical genome science" from the Ministry of Education, Culture, Sports, Science and Technology of Japan.

References

1. Katz A.M. (1990) Cardiomyopathy of overload. a major determinant of prognosis in congestive heart failure. N Engl J Med;322:100–110.
2. Frey N., Olson E.N. (2003) Cardiac hypertrophy: the good, the bad, and the ugly. Annu Rev Physiol;65:45–79.
3. Frey N., McKinsey T.A., Olson E.N. (2000) Decoding calcium signals involved in cardiac growth and function. Nat Med;6:1221–1227.
4. Wilkins B.J., Molkentin J.D. (2004) Calcium-calcineurin signaling in the regulation of cardiac hypertrophy. Biochem Biophys Res Commun;322:1178–1191.
5. Sussman M.A., Lim H.W., Gude N., Taigen T., Olson E.N., Robbins J., Colbert M.C., Gualberto A., Wieczorek D.F., Molkentin J.D. (1998) Prevention of cardiac hypertrophy in mice by calcineurin inhibition. Science;281:1690–1693.
6. Luo Z., Shyu K.G., Gualberto A., Walsh K. (1998) Calcineurin inhibitors and cardiac hypertrophy. Nat Med;4:1092–1093.
7. Meguro T., Hong C., Asai K., Takagi G., McKinsey T.A., Olson E.N., Vanter S.F. (1999) Cyclosporine attenuates pressure-overload hypertrophy in mice while enhancing susceptibility to decompensation and heart failure. Circ Res;84:735–740.
8. Molkentin J.D., Lu J.-R., Antos C.L., Markham B., Richardson J., Robbins J., Grant S.R., Olson E.R. (1998) A Calcineurin-dependent transcriptional pathway for cardiac hypertrophy. Cell;93:215–228.
9. Rao A., Luo C., Hogan P.G. (1997) Transcriptional factors of the NFAT family: regulation and function. Annu Res Immunol;15:707–747.
10. Crabtree G.R. (1999) Generic signals and specific outcomes: signaling through Ca^{2+}, calcineurin, and NF-AT. Cell;96:611–614.
11. Platz K.P., Mueller A.R., Blumhardt G., Bachmann S., Bechstein W.O., Kahl A., Neuhaus P. (1994) Nephrotoxicity following orthotopic liver transplantation. A comparison between cyclosporine and FK506. Transplantation;58:170–178.
12. Hojo M., Morimoto T., Maluccio M., Asano T., Morimoto K., Lagman M., Shimbo T., Suthanthiran M. (1999) Cyclosporine induces cancer progression by a cell-autonomous mechanism. Nature;397:530–534.
13. Aramburu J., Yaffe M.B., Lopez-Rodriguez C., Cantley L.C., Hogan P.G., Rao A. (1999) Affinity-driven peptide selection of an NFAT inhibitor more selective than cyclosporin A. Science;285:2129–2133.
14. Pu W.T., Ma Q., Izumo S. (2003) NFAT transcription factors are critical survival factors that inhibit cardiomyocyte apoptosis during phenylephrine stimulation in vitro. Circ Res;92:725–731.
15. Noguchi H., Matsushita M., Okitsu T., Moriwaki A., Tomizawa K., Kang S., Li S.T., Kobayashi N., Matsumoto S., Tanaka K., Tanaka N., Matsui H. (2004) A new cell-permeable peptide allows successful allogeneic islet transplantation in mice. Nat Med;10:305–309.
16. Lindgren M., Hällbrink M., Prochiantz A., Langel Ü. (2000) Cell-penetrating peptides. Trends Pharmacol Sci;21:99–103.
17. Schwarze S.R., Dowdy S.F. (2000) In vivo protein transduction: intracellular delivery of biologically active proteins, compounds and DNA. Trends Pharmacol Sci;21: 45–48.
18. Gallouzi I.E., Steitz J.A. (2001) Delineation of mRNA export pathways by the use of cell-permeable peptides. Science;294:1895–1901.
19. Zhu J., McKeon F. (1999) NF-AT activation requires suppression of Crm1-dependent export by calcineurin. Nature;398:256–260.
20. Burkard N., Becher J., Heindl C., Neyses L., Schuh K., Ritter O. (2005) Targeted proteolysis sustains calcineurin activation. Circulation;111:1045–1053.
21. Matsushita M., Matsui H. (2005) Protein transduction technology. J Mol Med;83:324–328.
22. Snyder E.L., Meade B.R., Saenz C.C., Dowdy S.F. (2004) Treatment of terminal peritoneal carcinomatosis by a transducible p53-activating peptide. PLoS Biol;2:E36.
23. Walensky L.D., Kung A.L., Escher I., Malia T.J., Barbuto S., Wright R.D., Wagner G., Verdine G.L., Korsmeyer S.J. (2004) Activation of apoptosis in vivo by a hydrocarbon-stapled BH3 helix. Science;305:1466–1470.

Available online at www.sciencedirect.com
ScienceDirect
Journal of Controlled Release 122 (2007) 159 – 164
journal of controlled release
www.elsevier.com/locate/jconrel

Development of bionanocapsules targeting brain tumors

Yumi Tsutsui [a], Kazuhito Tomizawa [a,*], Mana Nagita [b], Hiroyuki Michiue [a], Tei-ichi Nishiki [a], Iori Ohmori [a], Masaharu Seno [c], Hideki Matsui [a]

[a] *Department of Physiology, Okayama University Graduate School of Medicine, Dentistry and Pharmaceutical Sciences, 2-5-1 Shikata-cho, Okayama 700-8558, Japan*
[b] *Beacle Inc., 2-10-13 Kadota-Bunka, Okayama 703-8273, Japan*
[c] *Department of Medical Bioengineering, Okayama University Graduate School, of Natural Science and Technology, 3-1-1 Tsushima-Naka, Okayama 700-8530, Japan*

Received 19 March 2007; accepted 19 June 2007
Available online 27 June 2007

Abstract

Bionanocapsules (BNCs) are hollow nanoparticles that are composed of L protein (the hepatitis B virus surface antigen) and show specific affinity for human hepatocytes. The pre-S1 peptide displayed on the surface of BNCs is the specific ligand for binding to the receptor on human hepatocytes. Therefore, BNCs are not delivered to other tissues, such as the brain. The aim of the present study was to develop a novel drug delivery system (DDS) targeting brain tumors using BNCs that selectively targeted brain tumors. Epidermal growth factor receptor (EGFR), especially a constitutively active genomic sequence deletion variant of EGFR (EGFRvIII), is overexpressed in human glioblastoma. In the present study, we replaced the pre-S1 peptide with the antibody affinity motif of protein A and made hybrid BNCs conjugated with anti-human EGFR antibody recognizing EGFRvIII. The hybrid BNCs were efficiently delivered to glioma cells but not normal glial cells. Moreover, we confirmed the specific delivery of the hybrid BNCs to brain tumors in an *in vivo* brain tumor model. These results suggest that this new approach using BNCs is a promising system for brain tumor-targeted drug delivery.

Keywords: Brain tumor; Drug delivery system (DDS); Gene therapy; Hepatitis virus B (HBV)

1. Introduction

The difficulties associated with treatment of malignant brain tumors such as glioblastoma are well documented. For example, local infiltration of high-grade glioblastomas prevents the complete resection of all malignant cells. Moreover, glioblastoma is resistant to radiation. Although surgery together with chemotherapy is generally performed for brain tumors, malignant brain tumors are the most lethal primary tumors with a median survival of less than 12 months because of the difficulty of the targeting of anti-tumor drugs to brain tumors [1]. Thus, it is critical to develop drug delivery systems (DDSs) for chemotherapeutic agents that destroy individual cancer cells without causing diffuse damage to surrounding brain tissues.

BNCs are composed of the surface antigen (sAg) of hepatitis B virus (HBV) [2]. BNCs are efficient nanomachines with which to incorporate various materials such as chemical compounds, proteins, genes and siRNA and to accomplish the liver-specific delivery of the materials [2]. BNCs are recombinant yeast-derived hepatitis B virus surface antigen particles, which have been used as a recombinant hepatitis B vaccine for the last 20 years throughout the world, suggesting that BNCs are a safe DDS. If BNCs can be specifically delivered to brain tumors, BNCs might be promising carriers of anti-tumor drugs to brain tumors and be effective for the treatment of brain tumors. Hepatitis B virus (HBV) is a human liver-specific virus whose 3.2-kilobase-pair genome harbors three overlapping envelope genes in a single open reading frame, encoding small (S), medium (M) and large (L) proteins [3]. BNCs have an average diameter of 80 nm and consist of about 110 molecules of L protein embedded in a yeast endoplasmic reticulum (ER) membrane-derived phospholipid vesicle, with no HBV

* Corresponding author. Tel.: +81 86 235 7109; fax: +81 86 235 7111.
E-mail address: tomikt@md.okayama-u.ac.jp (K. Tomizawa).

0168-3659/$ - see front matter © 2007 Elsevier B.V. All rights reserved.
doi:10.1016/j.jconrel.2007.06.019

genome inside [2]. L protein contains Pre-S1 peptide, the N-terminal amino acid residues 108–119, which is displayed on the surface of BNCs and HBV L particles and functions as the specific ligand for binding to receptors on human hepatocytes and is crucial for HBV infectivity [4]. These results suggest that deletion of the pre-S1 peptide would abolish the targeting to hepatocytes, and that the replacement of the pre-S1 peptide with a targeting molecule for brain tumors would be effective for targeting to brain tumors.

EGFR is overexpressed in a variety of human malignancies of epithelial origin, particularly in the cancers of the brain, lung, colon, and head and neck [5,6]. Moreover, gliomas often express EGFRvIII, a constitutively active genomic sequence deletion variant of EGFR [7–11]. This variant of EGFR strongly and persistently activates the phosphatidylinositol 3′ kinase (PI3K) signaling pathway, which provides critical information for cell survival, proliferation and motility [12–16]. These results suggest that BNCs conjugated with anti-human EGFR antibody that recognizes EGFRvIII would be capable of targeting brain tumors.

In the present study, the pre-S1 peptide on the surface of BNCs was replaced with the antibody affinity motif of protein A binding anti-human EGFR antibody to produce "hybrid BNCs". The hybrid BNCs were specifically delivered to cultured glioma cells but not normal glial cells. Moreover, the targeting to glioma was confirmed in a mouse brain tumor model.

2. Materials and methods

2.1. Preparation of hybrid BNCs

The pre-S1 region of L protein, which composes BNCs [2], was replaced with an IgG Fc binding motif, the so-called ZZ-tag, which is the two-helix domain of protein A derived from *Staphylococcus aureus* [17] as described previously [2]. For conjugation with rhodamin B isothiocyanate (RITC) and anti-EGFR antibody, BNCs were incubated with RITC (1 mg/mL) at room temperature for 15 min and the mixture was further reacted at 4 °C overnight in PBS containing 3.4 mM EDTA (PBSE, pH 8–9). The mol ratio of RITC to BNC was 110 to 1. After incubation, BNCs were incubated with ethanolamine

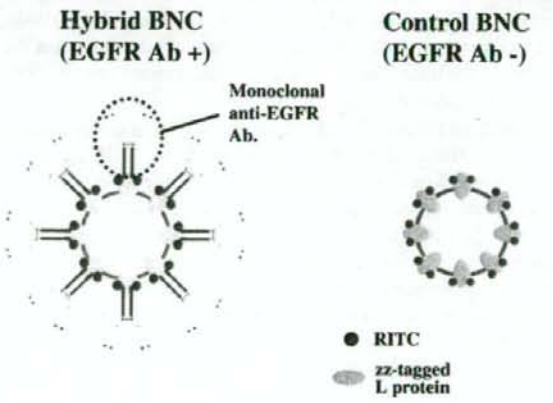

Fig. 1. Scheme of components of hybrid BNCs and control BNCs. Monoclonal anti-EGFR antibody is conjugated with BNC through protein A in hybrid BNC.

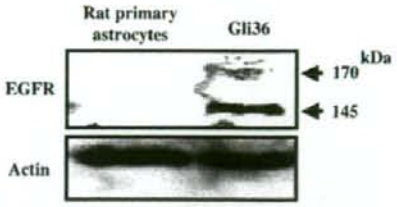

Fig. 2. Specificity of anti-EGFR antibody against EGFRvIII. The cell lysates of rat primary astrocytes and Gli36 cells were used for Western blotting analysis for EGFR (wild-type and vIII) and actin.

(final concentration, 2.5 mM) for 2 h at 4 °C to inactivate non-reactants. The buffer solution of the BNCs was then replaced by PBSE using a PD10 column. The RITC-conjugated BNCs were mixed with monoclonal anti-EGFR antibodies prepared from the hybridoma HB-9764 (ATCC, VA) at a ratio of BNC-RITC to EGFR antibody of 1 to 110 (mol/mol) for 1 h at 4 °C (hybrid BNC, Fig. 1). As a control, RITC-conjugated BNCs without anti-EGFR antibodies were used (Fig. 1).

2.2. Human glioma cell culture

For all experiments, human glioma cell line Gli36 (a gift from Dr. E.A. Chiocca, Massachusetts General Hospital, Boston, MA) was used. The cell expresses EGFRvIII but not wild-type EGFR. The cells were maintained in Dulbecco's modified Eagle's medium (DMEM) (GIBCO) supplemented with 10% (vol/vol) fetal bovine serum at 37 °C in a humidified atmosphere containing 5% carbon dioxide/95% air.

2.3. Primary culture of astrocytes

Rat primary astrocytes were prepared from newborn Wistar rats. The cortexes of the rats on postnatal day 1 were dissected, and the meninges were removed. The cortical tissues were then treated with 0.25% trypsin-ED TA (Invitrogen, Carlsbad, CA, USA) for 15 min at 37 °C and further treated with 0.004% DNase-I (Sigma-Aldrich Chemical, St. Louis, MO, USA) for 10 min. The pieces of the cortex were mechanically dissociated. The dissociated cells were plated onto collagen-coated 10-cm dishes. The plated cell density was approximately 150,000 cells/ml. The cells were maintained in DMEM with 10% fetal bovine serum (FBS) and 5% horse serum at 37 °C in a 95% air, 5% CO_2 humidified incubator.

2.4. Western blotting analysis

Western blotting analysis was performed as described previously [18]. Briefly, the harvested cells were homogenized by sonication in a boiling buffer containing 1% SDS. Samples were resolved by SDS-PAGE and then transferred to nitrocellulose membranes (Hybond ECL, GE Healthcare, Chalfont St., Giles, UK). The blots were probed with primary antibody against EGFR (1:3000 dilution, 101-7300-0, Katayama Chemical Inc.) and were visualized with an enhanced chemiluminescence detection system (Amersham Biosciences).

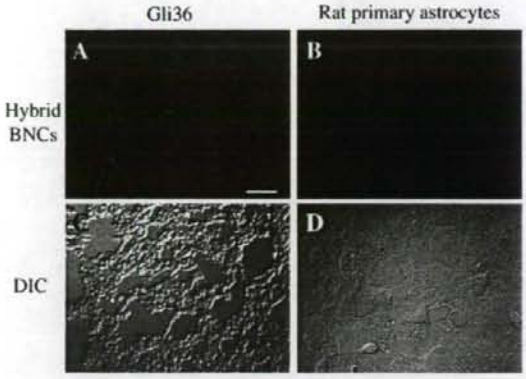

Fig. 3. Uptake of EGFR antibody-conjugated RITC-labeled BNCs (hybrid BNC) in Gli36 cells and rat primary astrocytes. Localization of hybrid BNCs in Gli36 cells (A) and rat astrocytes (B). C and D, DIC image. Bar=100 μm.

2.5. Confocal imaging of hybrid BNCs

To observe the delivery of BNCs to glioma cells, Gli36 cells were plated on 35-mm glass-bottom dishes coated with poly-L-lysine (Sigma-Aldrich Chemical) and collagen. The plated cell density was approximately 150,000 cells/ml. The cells were maintained in Dulbecco's modified Eagle's medium supplemented with FBS and cultured in a 37 °C incubator with 5% CO_2 for 24 h. Cells were then treated with concentrations of hybrid BNCs or control BNCs. After 4 h, the cells were washed 3 times with fresh medium and RITC signals on BNCs were then observed using a confocal laser microscope (FluoView 300, Olympus, Tokyo, Japan).

2.6. In vivo experiment

Gli36 cells (2×10^5 number) were implanted in the striatum of male 4-to-6-week-old nude mice (BALB/c-nu/nu, Japan SLC) as previously described [19]. Briefly, the mice were placed in a stereotactic device and implanted with a guide screw canula (Plastics One Inc., Roanoke, VA, USA) into the right striatum (1 mm anterior, 2.0 mm lateral, and 3.0 mm ventral to the bregma) under anesthesia with nembutal (50 mg/kg). Gli36 cells were resuspended in 2 μl of PBS and were injected using a 26-gauge needle and a Hamilton syringe through the guide canula in the mice.

After 2 weeks, mice were injected with 2 μl of hybrid BNCs (65.6 ng/μl EGFR antibody) or control BNCs through the guide screw canula. After 4 h, the mice were killed and fixed with 4% parafolmaldehyde. After fixation, the brains were placed in 10% sucrose/20% sucrose/30% sucrose successively after saturation had been achieved. Brains sections of 25-μm thickness were cut on a microtome (CM 1850, Leica Microsystems, Wetzlar, Germany). The RITC signals in the sections were observed using a confocal laser microscope (FluoView 300), and then the sections were stained with hematoxylin and eosin for detection of the brain tumor.

3. Results

3.1. In vitro delivery of hybrid BNCs

To confirm the specificity of the anti-EGFR antibody for EGFRvIII, Western blotting analysis was performed. Gli36 cells express EGFRvIII (145 kDa), whereas primary cultured rat astrocytes do not express EGFRvIII and express a low level of wild-type EGFR (170 kDa). The antibody detected EGFRvIII in Gli36 cells but did not detect any EGFR in normal rat astrocytes (Fig. 2).

To investigate the targeting of hybrid BNCs conjugated with the anti-EGFR antibody to glioma cells, Gli36 cells and rat primary astrocytes were incubated with 1.1 μg/ml hybrid BNCs. The targeting of BNCs was evaluated by detecting the fluorescence of RITC conjugated with the BNCs using confocal laser microscopy. Punctate fluorescence of the hybrid BNCs was observed in almost all Gli36 cells when they were incubated with 1.1 μg/ml BNCs (Fig. 3). In contrast, the signal of hybrid BNCs

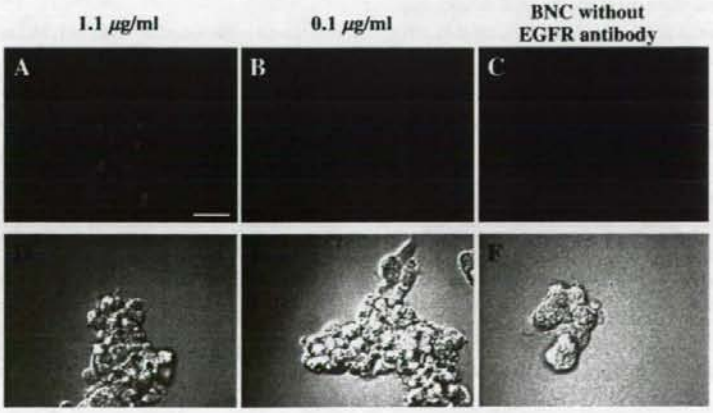

Fig. 4. Dose-dependent effect of hybrid BNCs on targeting to Gli36 cells. A, B and C, BNC localization; D, E and F, DIC image. A and B, hybrid BNCs; C, control BNCs (minus anti-EGFR antibody). Bar=50 μm.

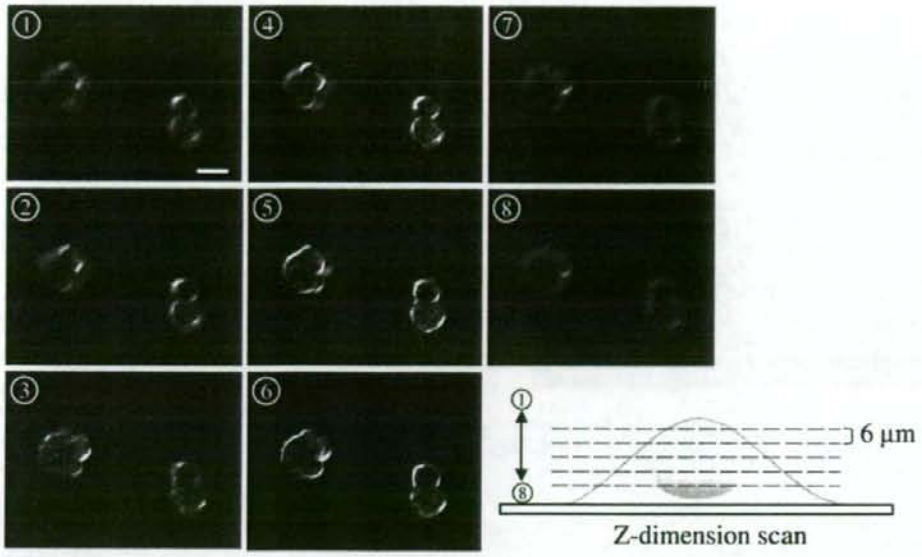

Fig. 5. Images of multiple optical 6-μm interval sections in a laser scan of the Z-dimension of Gli36 cells. Bar=20 μm.

was under the limit of detection in normal astrocytes (Fig. 3). We also examined the dose-dependency of the delivery of hybrid BNCs to Gli36 cells. The total amount of hybrid BNCs delivered to Gli36 cells using low-dose hybrid BNCs (0.1 μg/ml) was lower than that delivered using high-dose (1.1 μg/ml) BNCs (Fig. 4). Moreover, BNCs without anti-EGFR antibody were not observed in Gli36 cells (Fig. 4). These results suggest that hybrid BNCs conjugated with anti-EGFR antibody are effectively delivered to glioma cells but not normal glial cells.

HBV is internalized into hepatocytes by receptor-mediated endocytosis [20]. To examine whether hybrid BNCs were internalized into glioma cells or localized on the surface of the cells, serial optical sections at 6-μm intervals along the Z-dimension of Gli36 cells incubated with BNCs were then examined with a confocal microscope. Most fluorescence signals of hybrid BNCs were observed in the cell bodies of the cells, and weak signals were seen on the surface of the cell membrane (Fig. 5). These results suggest that hybrid BNCs were internalized into glioma cells.

There are two possibilities regarding the mechanism of the internalization of hybrid BNCs in glioma cells. One possibility is that the hybrid BNCs are internalized through EGF receptor-mediated enodocytosis after binding of anti-EGFR antibody to the EGF receptor. Another possibility is that BNCs themselves have the ability to be internalized in cells after binding to the cell surface. To examine the mechanism of internalization of hybrid BNCs, anti-EGFR antibody was conjugated with green fluorescent protein (GFP), and Gli36 cells were incubated with the GFP-fused antibody for 4 h. GFP signals were then observed by confocal microscopy. Anti-EGFR antibody was localized on the surface, and internalization of the fusion protein was not observed in Gli36 cells (Fig. 6).

3.2. *In vivo delivery of BNCs*

To investigate whether hybrid BNC targets brain tumors, we examined the efficiency of the delivery of hybrid BNCs in a mouse model of brain tumors. In the control BNC-injected

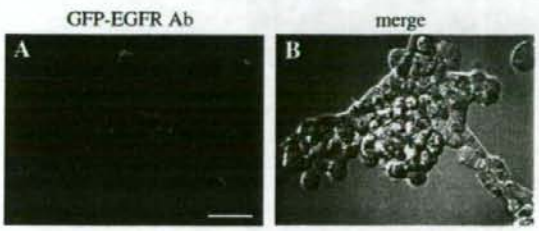

Fig. 6. Localization of anti-EGFR antibody in Gli36 cells. Gli36 cells were incubated with anti-EGFR antibody conjugated with GFP. A, GFP signals; B, Merged image with DIC. Bar=50 μm.

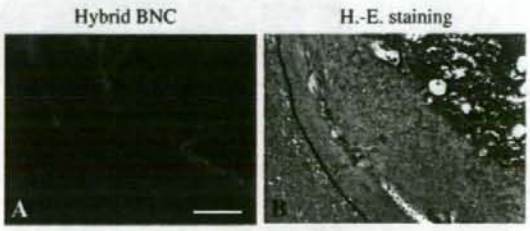

Fig. 7. Localization of hybrid BNCs in a mouse brain tumor model. A, localization of hybrid BNC in brain tumor. B, H.E. staining of the same section as in A. *, necrotic brain tumor. Black line in B represents the border between tumor and normal brain tissues. Bar=500 μm.

mouse brain, there was no detection of BNCs in either the brain tumor tissues or normal brain tissues (data not shown). In contrast, strong signals of hybrid BNCs were observed in the brain tumor tissue, but not in normal brain tissues (Fig. 7).

4. Discussion

Bionanocapsules (BNCs) have been developed as a DDS for living human cells [2]. BNCs are efficient nanomachines for achieving liver-specific delivery of genes and drugs [2,21]. BNCs have the same tissue-specific infectivity as HBV, because they both contain the N-terminal region of L protein, pre-S1, which specifies a narrow host range and distinct organ tropism. The region of amino acid residues 3 to 77 of pre-S1 is essential for this specificity [22]. In the present study, the pre-S1 region of BNCs was replaced with protein A and conjugated with anti-EGFR antibody. The resultant hybrid BNCs were targeted to glioma cells, but not normal glial cells or other normal tissues. These results suggest that replacement of the pre-SI region with other targeting moieties or biorecognition molecules, such as antibodies, receptors and ligands, may be applicable for the retargeting of BNCs to specific cells or tissues other than liver tissue.

The gene encoding EGFR is often amplified or mutated in human gliomas, but its expression is low or undetectable in the normal brain [8,23]. Based on this, EGFRvIII, a mutant isoform of EGFR, is under intensive investigation as a molecular target for the specific delivery of diagnostic and therapeutic agents to brain tumors [24]. In the present study, BNCs were conjugated with anti-EGFR antibody that recognized EGFRvIII, and the hybrid BNCs were specifically delivered to glioma cells both *in vitro* and *in vivo*. These results suggest that EGFRvIII is a promising molecular target for specific delivery of anti-cancer agents to malignant brain tumors.

5. Conclusions

In the present study, we developed a novel DDS targeting brain tumors using hybrid BNCs that selectively targeted brain tumors. Epidermal growth factor receptor (EGFR) is over-expressed in human gliomas, and hybrid BNCs containing anti-human EGFR antibody were efficiently delivered to glioma cells but not normal glial cells. Moreover, we confirmed the specific delivery of the hybrid BNCs to brain tumors in an *in vivo* model of brain tumors. These results suggest that this new approach using BNCs is a promising brain tumor-targeting drug delivery system.

Acknowledgement

This work was supported by the Research Program on Development of Innovative Technology from the Japan Science and Technology Agency (JST), by a grant from the New Energy and Industrial Technology Development Organization (NEDO), by a Grant-in-Aid for Scientific Research from the Ministry of Education, Science, Sports and Culture of Japan and by a Grant-in Aid for Scientific Research from the Ministry of Health, Labour and Welfare of Japan.

References

[1] S. Bao, Q. Wu, R.E. McLendon, Y. Hao, Q. Shi, A.B. Hjelmeland, M.W. Dewhirst, D.D. Bigner, J.N. Rich, Glioma stem cells promote radioresistance by preferential activation of the DNA damage response, Nature 444 (2006) 756–760.

[2] T. Yamada, Y. Iwasaki, H. Tada, H. Iwabuki, M.K. Chuah, T. VandenDriessche, H. Fukuda, A. Kondo, M. Ueda, M. Seno, K. Tanizawa, S. Kuroda, Nanoparticles for the delivery of genes and drugs to human hepatocytes, Nat. Biotechnol. 21 (2003) 885–890.

[3] K.H. Heermann, U. Goldmann, W. Schwartz, T. Seyffarth, H. Baumgarten, W.H. Gerlich, Large surface proteins of hepatitis B virus containing the pre-s sequence, J. Virol. 52 (2) (1984) 396–402.

[4] P.L. Marion, F.H. Salazar, J.J. Alexander, W.S. Robinson, Polypeptides of hepatitis B virus surface antigen produced by a hepatoma cell line, J. Virol. 32 (1979) 796–802.

[5] J. Mendelsohn, J. Baselga, The EGF receptor family as targets for cancer therapy, Oncog. Rev. 19 (56) (2000) 6550–6565.

[6] C.L. Arteaga, Overview of epidermal growth factor receptor biology and its role as a therapeutic target in human neoplasia, Semin. Oncol. Rev. 29 (2002) 3–9.

[7] K.D. Aldape, K. Ballman, A. Furth, J.C. Buckner, C. Giannini, P.C. Burger, B.W. Scheithauer, R.B. Jenkins, C.D. James, Immunohistochemical detection of EGFRvIII in high malignancy grade astrocytomas and evaluation of prognostic significance, J. Neuropathol. Exp. Neurol. 63 (7) (2004) 700–707.

[8] L. Frederick, X.Y. Wang, G. Eley, C.D. James, Diversity and frequency of epidermal growth factor receptor mutations in human glioblastomas, Cancer Res. 60 (5) (2000) 1383–1387.

[9] A.J. Wong, J.M. Ruppert, S.H. Bigner, C.H. Grzeschik, P.A. Humphrey, D.S. Bigner, B. Vogelstein, Structural alterations of the epidermal growth factor receptor gene in human gliomas, Proc. Natl. Acad. Sci. U. S. A. 89 (7) (1992) 2965–2969.

[10] N. Sugawa, A.J. Ekstrand, C.D. James, V.P. Collins, Identical splicing of aberrant epidermal growth factor receptor transcripts from amplified rearranged genes in human glioblastomas, Proc. Natl. Acad. Sci. U. S. A. 87 (21) (1990) 8602–8606.

[11] A.J. Ekstrand, C.D. James, W.K. Cavenee, B. Seliger, R.F. Pettersson, V.P. Collins, Genes for epidermal growth factor receptor, transforming growth factor alpha, and epidermal growth factor and their expression in human gliomas in vivo, Cancer Res. 51 (8) (1991) 2164–2172.

[12] R. Sordella, D.W. Bell, D.A. Haber, J. Settleman, Gefitinib-sensitizing EGFR mutations in lung cancer activate anti-apoptotic pathways, Science 305 (5687) (2004) 1163–1167.

[13] G. Choe, S. Horvath, T.F. Cloughesy, K. Crosby, D. Seligson, A. Palotie, L. Inge, B.L. Smith, C.L. Sawyers, P.S. Mischel, Analysis of the phosphatidylinositol 3′-kinase signaling pathway in glioblastoma patients in vivo, Cancer Res. 63 (11) (2003) 2742–2746.

[14] B. Li, M. Yuan, I.A. Kim, C.M. Chang, E.J. Bernhard, H.K. Shu, Mutant epidermal growth factor receptor displays increased signaling through the phosphatidylinositol-3 kinase/AKT pathway and promotes radioresistance in cells of astrocytic origin, Oncogene 23 (26) (2004) 4594–4602.

[15] H.S. Huang, M. Nagane, C.K. Klingbeil, H. Lin, R. Nishikawa, X.D. Ji, C.M. Huang, G.N. Gill, H.S. Wiley, W.K. Cavenee, The enhanced tumorigenic activity of a mutant epidermal growth factor receptor common in human cancers is mediated by threshold levels of constitutive tyrosine phosphorylation and unattenuated signaling, J. Biol. Chem. 272 (5) (1997) 2927–2935.

[16] S.K. Batra, S. Castelino-Prabhu, C.J. Wikstrand, X. Zhu, P.A. Humphrey, H.S. Friedman, D.D. Bigner, Epidermal growth factor ligand-independent, unregulated, cell-transforming potential of a naturally occurring human mutant EGFRvIII gene, Cell Growth Differ. 6 (10) (1995) 1251–1259.

[17] K.L. Witkin, R. Prathapam, K. Collins, Positive and negative regulation of tetrahymena telomerase holoenzyme, Mol. Cell. Biol. 27 (6) (2007) 2074–2083.

[18] K. Tomizawa, N. Iga, Y.F. Lu, A. Moriwaki, M. Matsushita, S.T. Li, O. Miyamoto, T. Itano, H. Matsui, Oxytocin improves long-lasting spatial memory during motherhood through MAP kinase cascade, Nat. Neurosci. 6 (2003) 384–390.